

## Disorder-induced Raman scattering in NiSi<sub>2</sub>

F. Li, N. Lustig, P. Klosowski, and J. S. Lannin

*Department of Physics, Penn State University, University Park, Pennsylvania 16802*

(Received 31 May 1989; revised manuscript received 16 January 1990)

Disorder-induced Raman scattering (DIRS) has been observed in epitaxial films of NiSi<sub>2</sub> on (111) Si. The DIRS, which is found to have primarily *A*-like symmetry, is attributed to Si-site disorder. A comparison with lower-resolution inelastic-neutron-scattering measurements on polycrystalline films suggests that the Raman spectra represent a coupling-parameter-weighted density of states.

### INTRODUCTION

Disorder in crystalline solids provides a means of modifying the  $k \approx 0$  selection rule for Raman scattering from periodic systems.<sup>1,2</sup> This disorder, which arises from nonperiodic perturbations of the crystalline lattice, may arise from a number of structural sources. This includes dilute impurity and alloy systems, isolated defects such as vacancies, defect complexes, and anharmonicity. In addition to these structural sources of disorder that yield significant local fluctuations in interatomic potential, mass variations may also result in disorder-induced Raman scattering (DIRS).<sup>2,3</sup> These structural sources provide a means of inducing spatially random polarizability derivative fluctuations that yield additional Raman activity for  $k \neq 0$  modes. In general, the presence of disorder associated with isolated defects results in Raman scattering that is a coupling-parameter-weighted, site-symmetry projection of the crystalline density of states. Under conditions of high-structural disorder, such as defect complexes or alloys, the DIRS may reflect the form of the phonon density of states. As in amorphous solids, the spectra may thus represent a coupling-parameter-weighted density of states.<sup>4</sup> Although information about the frequency variation of the coupling parameter  $\tilde{C}(\omega)$  has been obtained for amorphous solids,<sup>5,6</sup> comparable analysis has not been performed for DIRS in crystalline solids.<sup>7</sup> In elemental amorphous systems,  $\tilde{C}(\omega)$  has been found to have a relatively monotonic frequency dependence.

While DIRS has been extensively studied both experimentally and theoretically in insulators and semiconductors, less is known in detail about DIRS in metals. In the most extensively studied transition-metal carbide system, TiC<sub>*x*</sub> ( $x < 1$ ), C vacancies result in DIRS for which the mean-square polarizability is comparable on both Ti and C sites.<sup>8</sup> A large number of vacancies and likely defect clustering in this system results in the DIRS being similar in form to the phonon density of states. Similar results have been obtained for a number of other transition-metal nitride and carbide systems.<sup>9</sup> In the present study we present Raman-scattering measurements on the metallic cubic fluorite system, NiSi<sub>2</sub>. This and other transition-metal disilicide systems are of some interest for their electronic properties. Transport measurements in

NiSi<sub>2</sub> indicate a somewhat higher resistivity than that of the related CoSi<sub>2</sub> structure.<sup>10</sup> This has been interpreted as due to substantial NiSi<sub>2</sub> nonstoichiometry associated with Si-site disorder.

In contrast to the electronic properties of NiSi<sub>2</sub>, little is known about its vibrational states. The fluorite structure of NiSi<sub>2</sub> has a single allowed  $k \approx 0$  Raman-active mode. As noted below, no evidence of a sharp, intense  $k = 0$  scattering found in ionic fluorides is observed. Rather, the Raman scattering is found to be broad in form, indicating predominant DIRS. This induced scattering is compared to lower-resolution inelastic neutron-scattering measurements. The latter yield a cross section and mass-weighted phonon density of states. Similarities between these two spectra for much of the frequency range suggest that the Raman scattering provides a higher-resolution representation of a weighted phonon density of states.

### EXPERIMENT

Raman-scattering measurements were performed at 300 K on NiSi<sub>2</sub> and CoSi<sub>2</sub> samples prepared in an ultrahigh vacuum by depositing 400 Å of Ni and 320 Å of Co on ordered-crystalline (111) Si surfaces that were subsequently annealed to 800 °C. The resulting films indicated from low-energy electron-diffraction (LEED) studies high-quality epitaxial (111) structures.<sup>11</sup> A third monochromator system and an additional laser rejection filter were employed to reduce the stray light. The stray-light background was estimated using a laser spike filter at the entrance slit of the monochromator. The excitation wavelength was 5145 Å. Given the relatively weak signal, and the presence of a single-crystalline surface, only selected polarization analysis of the scattered light was performed. Measurements for the incident field,  $\vec{e}_i$ , along  $[\bar{1}10]$  and  $[\bar{1}\bar{1}2]$  and scattered fields,  $\vec{e}_s$ , along  $[\bar{1}10]$  were employed. Polarization unanalyzed (*U*) measurements for incident radiation in the horizontal scattering plane (*H*) are labeled here as *HU*. These spectra represent linear combinations of *HH* and *HV* scattering, where *V* represents fields perpendicular (vertical) to the scattering plane. For the present grating system and wavelength the *H* transmission is approximately a factor of 2 greater than the *V*. Spectroscopic ellipsometry measurements of

the NiSi<sub>2</sub> film indicate that at 5145 Å the derivatives of the real and imaginary parts of the dielectric constant are small, particularly the imaginary part. This demonstrates within a simple two-band resonance Raman theory<sup>12</sup> that, in contrast to the case of TiC<sub>x</sub>, resonance enhancement is weak.

Inelastic neutron spectra were performed on the LER-MECS instrument at the Argonne National Laboratory Intense Pulsed Neutron Source (IPNS), Argonne, IL. Polycrystalline powder of NiSi<sub>2</sub>, obtained from Alpha Inorganic, of 99.9% purity was employed. The wavevector dependence of the scattering indicated similar forms of the modified dynamical structure factor for  $Q = 4.5 - 9.5 \text{ \AA}^{-1}$ .<sup>13</sup>

## RESULTS AND DISCUSSION

### DIRS and inelastic neutron scattering

The Raman spectrum of NiSi<sub>2</sub> is shown in Fig. 1 for *HU* scattering. Quite similar, though noisier *HH* spectra were obtained. In contrast, the *VH* component did not yield any significant scattering above background. The sharp feature at 521 cm<sup>-1</sup> is due to first-order scattering from the Si substrate; contributions from second-order Si scattering are weak for this configuration. For the (111) crystal face the first-order  $k \approx 0$  scattering from  $T_{2g}$  modes of NiSi<sub>2</sub> is allowed for all polarization configurations. These modes only involve Si motions. Nonetheless, as shown in Fig. 1, no sharp  $k \approx 0$  feature is observed. In contrast, the spectra of Fig. 1 indicate several broad features attributed to DIRS. In CoSi<sub>2</sub>, a single, very weak, narrow  $k \approx 0$  attributed scattering is observed at 267 cm<sup>-1</sup>. Given the similar mass of Co and Ni and the slightly larger (0.6%) first-neighbor distance in NiSi<sub>2</sub>, a correspondingly weak  $k \approx 0$  peak at a somewhat lower frequency is expected. It is possible that this peak is masked by disorder-induced scattering near 230 cm<sup>-1</sup>.

The DIRS observed in Fig. 1 is attributed to the presence of Si-site disorder associated with either or both Ni-antisite defects on Si sites or the presence of Si vacancies. For an isolated Si-site defect, polarizability fluctuations would yield a linear combination of scattering from  $A_1$ ,  $E$ , and  $T_2$  combinations. For the *VH* component with

$\bar{e}_i \parallel [\bar{1}12]$  and  $\bar{e}_s \parallel [\bar{1}\bar{1}0]$  this yields the combination  $E + \frac{2}{3}T_2$ . The weakness of the *VH* scattering implies that the contribution of the  $E$  and  $T_2$  components is small. The *HH* scattering for  $\bar{e}_i \parallel [\bar{1}10]$  and  $\bar{e}_s \parallel [\bar{1}10]$  yields for isolated defects a contribution of  $A_1 + E + T_2$ . The Raman results thus indicate that *HH* scattering is the dominant contribution to the polarization unanalyzed spectra of Fig. 1. The absence of *VH* scattering within our signal-to-noise ratio suggests that the disorder-induced scattering is primarily due to " $A_1$ " scattering. This result contrasts with disorder-induced scattering in transition-metal carbides for which " $A$ " and " $E$ " components of the scattering contribute comparable contributions.<sup>7</sup> However, defect clustering, suggested below, may formally invalidate a single-site symmetry analysis. The use of symmetry symbols such as " $A$ " is a representation of this possibility.

The origin of the disorder-induced scattering in *c*-NiSi<sub>2</sub> is likely to arise from the Si-site disorder associated with the nonstoichiometry of this material. Various references suggest that the actual composition corresponds to Ni<sub>1.04</sub>Si<sub>1.92</sub>.<sup>14</sup> Diffraction measurements have suggested that the Si-site disorder is associated both with  $\sim 1.4\%$  Si vacancies as well as  $\sim 2\%$  antisite defects due to Ni atoms on Si sites. This disorder, which has been suggested to explain the higher resistivity of the NiSi<sub>2</sub> system relative to stoichiometric CoSi<sub>2</sub>,<sup>10</sup> is thus the likely origin of the disorder-induced scattering. The presence of vacancies and antisite defects at the level of 3.4% of the Si lattice sites implies, as does the TiC<sub>x</sub> system, that clustering of such defects may occur. Clustering corresponds to defects that are spatially separated by small distances, such as first- or second-neighbor defect sites.

The Si sites in CaF<sub>2</sub> structures form a simple-cubic lattice with six first neighbors and eight second neighbors. The probability  $P_i$  that a defect site has only one defect neighbor for random-site occupancy is  $n_i [\mathcal{C}] [1 - \mathcal{C}]^{n_i - 1}$ , where  $n_i$  is the number of *i*th neighbors and  $[\mathcal{C}]$  the concentration of defects. For the CaF<sub>2</sub> structure with  $[\mathcal{C}] = 0.034$ ,  $P_1 = 0.17$  and  $P_2 = 0.21$ . Thus for random occupancy there is a 38% probability of first and second neighbors forming defect clusters. If clustering is non-random, and the system tends form defect clusters, these values serve as lower limits for  $[\mathcal{C}] = 0.034$ . As detailed structural studies have not been performed on the present films, we implicitly assumed a 3.4% defect concentration. It is possible, however, that the concentration of defects in the present epitaxial films is lower than this number. It is useful to note that nonrandom clustering of anion vacancies has also been suggested to occur in ionic oxides with the CaF<sub>2</sub> structure.<sup>15</sup>

The distinct, broad bands of the spectrum in Fig. 1 suggest that it may represent a weighted phonon density of states. In elemental amorphous solids, the thermally reduced Raman spectra  $I/(n+1)$  yield a better approximation to the form of the phonon density of states than either  $I$  or the reduced intensity  $I\omega/(n+1)$ . This is due to frequency-dependent coupling-parameter variations.<sup>16</sup> Shown in Fig. 2 is the thermally reduced spectrum of Fig. 1 after subtraction of the stray light and Si-substrate

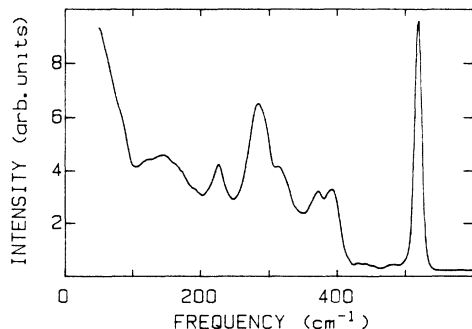


FIG. 1. Raman spectrum (*HU*) of NiSi<sub>2</sub>.

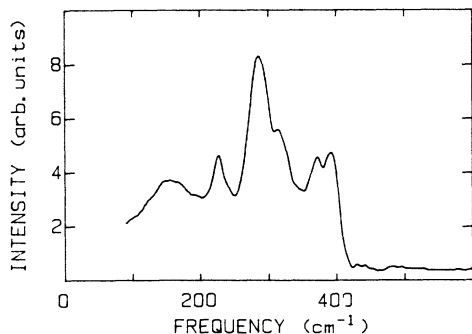


FIG. 2. Thermally reduced *HU* Raman spectrum,  $I/(n+1)$ , of  $\text{NiSi}_2$ .

background. Given the predominant “*A*” character of this scattering, it is of interest to determine whether it represents the major features of the phonon density of states. To determine if this is the case, a comparison is made in Fig. 3 with inelastic neutron-scattering measurements performed on polycrystalline powder of  $\text{NiSi}_2$ . A more detailed discussion of the neutron measurements and the associated wave-vector averaging employed to determine  $G(\omega)$  are presented elsewhere.<sup>13</sup> The neutron spectra, represented by the dynamical scattering function  $G(\omega)$ , are proportional to a weighted density of states through the relation<sup>17</sup>

$$G(\omega) \sim \sum_i w_i g_i(\omega) = w_{\text{Ni}} g_{\text{Ni}}(\omega) + w_{\text{Si}} g_{\text{Si}}(\omega). \quad (1)$$

Here  $g_i(\omega)$  are the individual contributions to  $g(\omega)$ , the total phonon density of states, and  $w_i$  the neutron weight-

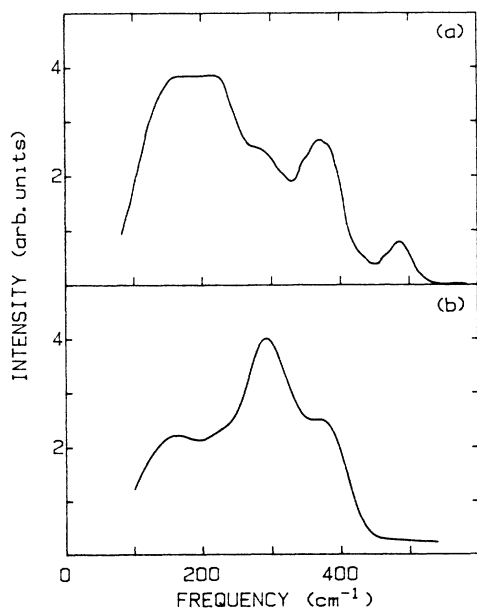


FIG. 3. Comparison of (a) inelastic neutron,  $G(\omega)$  spectrum and (b) thermally reduced Raman spectrum of  $\text{NiSi}_2$ . The Raman spectrum has been broadened by a neutron resolution of  $48 \text{ cm}^{-1}$ .

ing factors;  $w_i = \sigma_i c_i / m_i$ , where  $\sigma_i$  is the coherent neutron cross section,  $m_i$  the atomic mass, and  $c_i$  the concentration of species  $i$ . Equation (1) assumes polarization and Debye-Waller factors do not significantly modify the frequency dependence of  $G(\omega)$ . For  $\text{NiSi}_2$  the weighting-factor ratio  $w_{\text{Ni}}/w_{\text{Si}} = 1.5$ , while the integrated contribution of Ni to Si modes to  $G(\omega)$  is approximately a factor of 2.8.

The resolution of these neutron measurements of  $\sim 48 \text{ cm}^{-1}$  is substantially below that of the Raman spectra ( $5 \text{ cm}^{-1}$ ). As such, the thermally reduced Raman spectra have been Gaussian broadened in Fig. 3(b) for comparison with the neutron measurements. The positions of the peaks in the neutron and broadened Raman spectra are mutually consistent, each reflecting the major features of the phonon density of states. For the inelastic neutron results, the larger Ni weighting factor for the low-frequency modes results, however, in a relatively larger scattering from the low-frequency band centered at  $192 \text{ cm}^{-1}$ . As the nonbroadened spectra in Fig. 2 imply, this band is composed of two unresolved features at  $130$  and  $225 \text{ cm}^{-1}$ . The major peak in the Raman spectra at  $290 \text{ cm}^{-1}$  is observed in the neutron data as a shoulder. This is attributed to the possible combined effects of an enhanced DIRS coupling parameter, a lower neutron weighting factor for modes involving Si motion, as well as an overlap with the lower-frequency band. The Raman spectra also indicate a weak shoulder at  $315 \text{ cm}^{-1}$ , while both Raman and neutron spectra indicate a distinct minimum at  $330 \text{ cm}^{-1}$ . The neutron peak at  $368 \text{ cm}^{-1}$  is also found to correspond to two features at  $372$  and  $392 \text{ cm}^{-1}$  in the higher-resolution DIR spectrum. Somewhat surprisingly, the highest neutron band at  $480 \text{ cm}^{-1}$  is not observed in the high-frequency Raman spectrum. The origin of either weak Raman scattering or an anomalous neutron peak is unexplained at this time. Measurements of tetragonal  $\text{WSi}_2$  do not exhibit a corresponding high-frequency peak in  $G(\omega)$ . It is possible that the  $480\text{-cm}^{-1}$  peak is associated with a contaminant phase of unknown origin.

The Raman spectra of Figs. 1 and 2 indicate five major bands within which some fine structure is suggested. Although the nature of the interactions in this metallic system involves both metallic and covalent bonding, its density of states appears in a very rough sense to have a form not unlike that of some ionic fluoride systems.<sup>17</sup> This broad similarity in terms of numbers of peaks may well be fortuitous, given the detailed differences in the dispersion curves for metallic systems. In particular, screening effects yield characteristically different dispersion relative to that of ionic materials.

The relatively high-scattering intensity for the low-frequency band in the inelastic neutron spectra of Fig. 3 is consistent with eigenvectors having predominant Ni-atom motion. In contrast, the scattering from the two highest bands in  $G(\omega)$  are likely to involve Si motions. It is thus reasonable to assume that contributions to the induced scattering involve both first-neighbor Ni atoms and second-neighbor Si atoms about the defect site. It is not possible (as in the  $\text{TiC}_x$  system) to assume very little metal-atom motion at high frequencies, given the smaller

mass ratio of  $\sim 2$  for  $\text{NiSi}_2$  versus 4 for  $\text{TiC}_x$ . It is reasonable, however, given the relative intensity of the high-frequency scattering, to assume significant contributions from polarizability fluctuations of Si atoms. Thus, it appears likely that polarizability fluctuations extend beyond first neighbors of the defect, either due to the nature of the electronic states of the atoms about the defect, or to vacancy or defect clusters.

### CONCLUSIONS

In summary, disorder-induced Raman scattering has been observed in epitaxial films of  $\text{NiSi}_2$  on a (111) Si substrate. The disorder has been attributed to Si-site disorder due to either or both vacancies or Ni-antisite defects. The allowed  $k \approx 0$  scattering is weak and not clearly observed; this is consistent with weak allowed scattering in ordered  $\text{CoSi}_2$ . A comparison with a lower-resolution in-

elastic neutron-scattering measurement of the weighted phonon density of states suggests that the Raman spectra also indicate a weighted, high-resolution form of the density of states. This result is similar to the effect of disorder in  $\text{TiC}_x$  and related carbides and nitrides. The primary " $A_1$ " character of the scattering differs, however, from that of  $\text{TiC}_x$ . Given its high resolution, the disorder-induced Raman measurements should provide useful information for theoretical studies of the phonon density of states of  $\text{NiSi}_2$  and other disilicides.

### ACKNOWLEDGMENTS

This work was supported by U.S. Department of Energy Grant No. DE-FG02-84ER45095. We wish to thank Dr. Yves J. Chabal and Dr. Julia M. Phillips for the  $\text{NiSi}_2$  and  $\text{CoSi}_2$  samples, respectively, and Dr. John C. Hensel for providing useful references on Si-site disorder.

<sup>1</sup>J. M. Worlock and S. P. S. Porto, Phys. Rev. Lett. **15**, 697 (1965).

<sup>2</sup>N. X. Xinh, in *Localized Excitations in Solids*, edited by R. F. Wallis (Plenum, New York, 1968), p. 167.

<sup>3</sup>J. S. Lannin, Phys. Rev. B **16**, 1510 (1977).

<sup>4</sup>R. Shuker and R. W. Gammon, Phys. Rev. Lett. **25**, 222 (1970).

<sup>5</sup>N. Maley and J. S. Lannin, Phys. Rev. B **35**, 2456 (1987).

<sup>6</sup>F. Li and J. S. Lannin, Phys. Rev. B **39**, 6220 (1989).

<sup>7</sup>The similar form of the Raman and neutron scattering of  $\text{TiC}_x$  at low frequency (Ref. 8) implies that the coupling parameter  $\tilde{C}(\omega)$  varies to first order as  $\omega/(n+1)$ , where  $n+1$  is the Bose-Einstein factor at 300 K.

<sup>8</sup>M. V. Klein, J. A. Holy, and W. A. Williams, Phys. Rev. B **17**, 1546 (1978).

<sup>9</sup>W. Spengler and R. Kaiser, Solid State Commun. **18**, 881 (1976).

<sup>10</sup>J. C. Hensel, in *Proceedings of the Materials Research Society*

(MRS, Pittsburgh, 1986), Vol. 54, p. 499.

<sup>11</sup>Y. J. Chabal, D. R. Hamann, J. E. Rowe, and M. Schlüter, Phys. Rev. B **25**, 7598 (1982).

<sup>12</sup>A. Pinczuk and E. Burnstein, in *Light Scattering in Solids I*, edited by M. Cardona (Springer-Verlag, New York, 1975), p. 64.

<sup>13</sup>P. Klosowski and J. S. Lannin, Solid State Commun. **72**, 927 (1989).

<sup>14</sup>For a review, see P. V. Geld and F. A. Sidorenko, *Silitsidi Perekhodnikh Metallov Chetvertogo Perioda* (Izdatelstvo Metallurgiya, Moscow, 1971).

<sup>15</sup>C. R. A. Catlow, in *Nonstoichiometric Oxides*, edited by O. T. Sorenson (Academic, New York, 1981), p. 61.

<sup>16</sup>J. S. Lannin, in *Semiconductors and Semimetals*, edited by J. I. Pankove (Academic, New York, 1984), Vol. 21B, p. 159.

<sup>17</sup>N. Lustig, J. S. Lannin, J. M. Carpenter, and R. Hasegawa, Phys. Rev. B **32**, 2778 (1985).